


Cite this: *RSC Adv.*, 2023, 13, 12869

Picolylamine–Ni(II) complex attached on 1,3,5-triazine-immobilized silica-coated Fe₃O₄ core/shell magnetic nanoparticles as an environmentally friendly and recyclable catalyst for the one-pot synthesis of substituted pyridine derivatives†

Sobhan Rezayati,^a Fatemeh Kalantari^a and Ali Ramazani *^{ab}

In the current study, an environmentally friendly and facile method was proposed for designing and constructing a catalyst with Ni(II) attached to a picolylamine complex on 1,3,5-triazine-immobilized Fe₃O₄ core-shell magnetic nanoparticles (Ni^{II}-picolylamine/TCT/APTES@SiO₂@Fe₃O₄) via a stepwise procedure. The as-synthesized nanocatalyst was identified and characterized via Fourier-transform infrared (FT-IR), X-ray photoelectron spectroscopy (XPS), thermogravimetric analysis (TGA), vibrating-sample magnetometry (VSM), transmission electron microscopy (TEM), X-ray diffraction (XRD), Brunauer–Emmett–Teller (BET), field-emission scanning electron microscopy (FE-SEM), inductively coupled plasma (ICP), and energy-dispersive X-ray spectrometry (EDX). The obtained results from the BET analysis indicated that the synthesized nanocatalyst had high specific area (53.61 m² g^{−1}) and mesoporous structure. TEM observations confirmed the particle size distribution was in the range 23–33 nm. Moreover, the binding energy peaks observed at 855.8 and 864.9 eV in the XPS analysis confirmed the successful and stable attachment of Ni(II) on the surface of the picolylamine/TCT/APTES@SiO₂@Fe₃O₄. The as-fabricated catalyst was used to produce pyridine derivatives by the one-pot pseudo-four component reaction of malononitrile, thiophenol, and a variety of aldehyde derivatives under solvent-free conditions or EG at 80 °C. The highest yield achieved was 97% for compound **4d** in EG at 80 °C with a TOF of 823 h^{−1} and TON of 107. It was found that the used catalyst was recyclable for eight consecutive cycles. On the basis of ICP analysis, the results indicated that the Ni leaching was approximately 1%.

Received 20th March 2023

Accepted 12th April 2023

DOI: 10.1039/d3ra01826a

rsc.li/rsc-advances

Introduction

The focus on sustainable chemistry and green chemistry in modern organic synthesis has intensified in recent years, and includes not using dangerous or toxic solvents and reagents, the avoidance of non-recyclable and expensive catalysts, and the avoidance of harsh reaction conditions.^{1–4} Over the past few decades, there has been increasing interest in the use of eco-friendly solvents or reagents, good atom economy, and measures that can save energy consumption in the synthesis of organic compounds.^{5–7} The use of clean and green chemical technologies both in organic transformations and in wider

industry still faces some significant challenges to produce valuable chemicals. One of the important factors in sustainable chemistry and green chemistry is the use of catalysts. Recently, research on catalysts, especially heterogeneous catalysts, in research transformations and in most chemical industrial processes has gained high significance. Likewise, for supporting the global community, catalysts can help the production of sustainable fuels and many indispensable chemicals.^{8–13} Therefore, efficient, green, and suitable catalysts have a great role to play in promoting sustainability. In this regard, nanocatalysts have many suitable unique features, including efficient recovery, low cost of production, excellent selectivity, high activity and stability, and good recyclability.

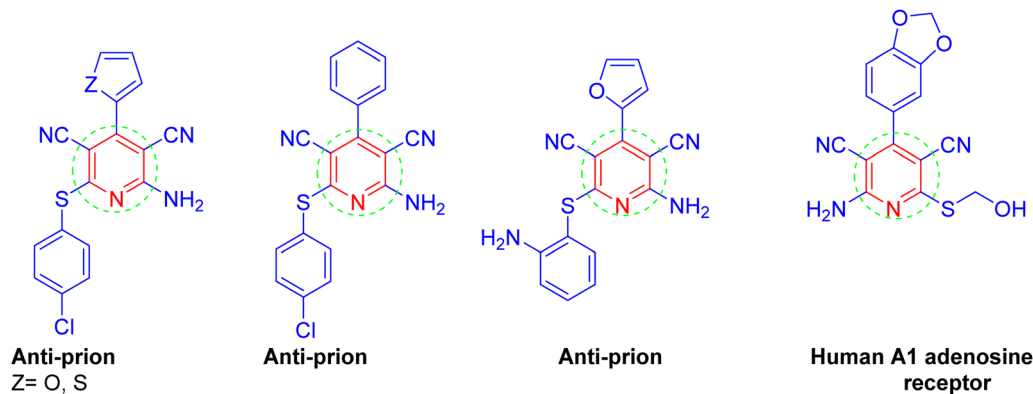
One of the most important modern science areas is nanoscience. Nanotechnology allows physicians, engineers, scientists, and chemists to do work at the cellular and molecular levels to make important advances in the healthcare and science fields, among others. In recent years, due to their electrical characteristics, distinctive magnetic properties, unique size, and high surface area, the utilization of magnetic nanoparticles (MNPs) has attracted considerable attention. They also

^aDepartment of Chemistry, Faculty of Science, University of Zanjan, Zanjan 45371-38791, Iran. E-mail: aliramazani@gmail.com; aliramazani@znu.ac.ir

^bDepartment of Biotechnology, Research Institute of Modern Biological Techniques (RIMBT), University of Zanjan, Zanjan 45371-38791, Iran

† Electronic supplementary information (ESI) available: Copies of FT-IR, ¹H NMR (250 MHz, CDCl₃ or DMSO-*d*₆) and ¹³C NMR (62.5 MHz, CDCl₃ or DMSO-*d*₆) spectra of the synthesized compounds, and XRD data for the Ni^{II}-picolylamine/TCT/APTES@SiO₂@Fe₃O₄. See DOI:

<https://doi.org/10.1039/d3ra01826a>

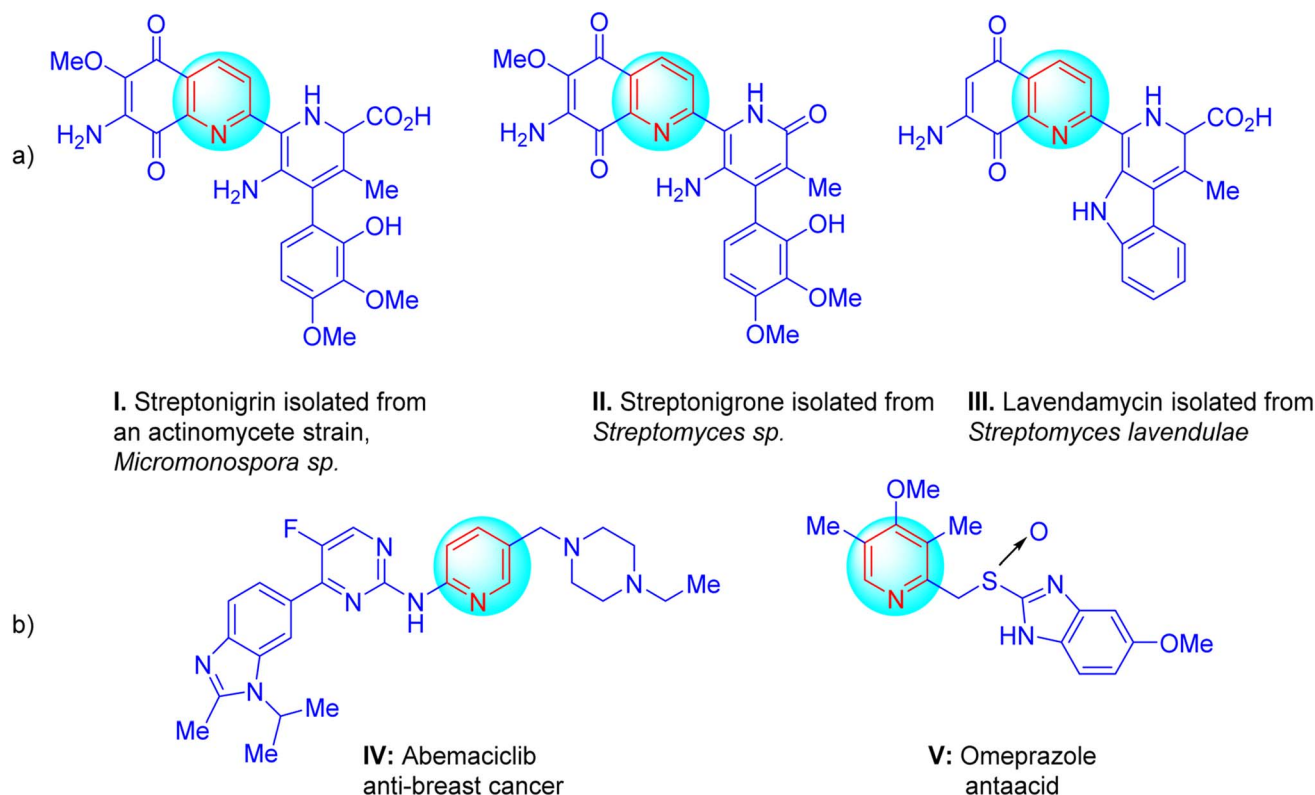



Scheme 1 Some biological pyridine derivatives.

have particular properties in industrial applications and biomedical applications, such as drug delivery systems, separation of metal ions for environmental remediation, bioisolation, saving information, biomolecular sensing, magneto-heat therapy, targeted gene therapy, and sensors.^{14–16} A high biocompatibility and sensitivity to postsynthetic surface functionalization have made magmite ($\gamma\text{-Fe}_2\text{O}_3$) and magnetite (Fe_3O_4) among the range of iron oxides, great candidates for many significant applications.^{17–22} One of the important advantages of MNPs as catalysts is their easy recovery using a magnetic field. The two intrinsic properties of paramagnetism and the insolubility of nanomagnets facilitate the separation of

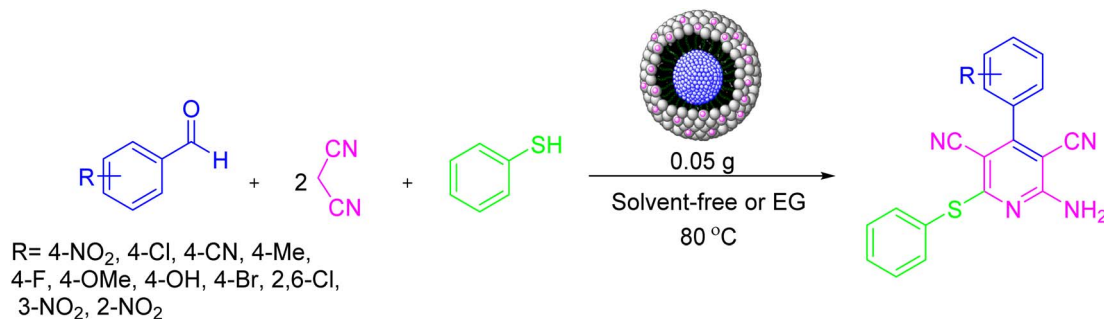
such magnetic catalysts from reaction mixtures. In particular, silica-modified MNPs have received widespread attention due to their various important advantages, such as ease and simplicity of synthesis, functionalization, and easy separation from the reaction medium employing a simple magnet, thermal stability, and low toxicity.

One of the best ways to synthesize new heterocyclic compounds from available and simple raw materials is through multicomponent reactions (MCRs), which have been widely employed in the preparation of biologically active molecules, natural products, and organic matter.^{23,24} The development of one-pot MCRs is one of the best methods for the synthesis of desired products due to certain



Scheme 2 (a) Some naturally occurring compounds (I, II, and III) bearing pyridine groups and (b) some drug molecules with a pyridine skeleton (IV and V).





Scheme 3 Activity of the Ni^{II}-picolylamine/TCT/APTES@SiO₂@Fe₃O₄ catalyst for the synthesis of substituted pyridine derivatives.

salient features of this method, such as high selectivity, facile automation, simplicity, and high atomic economy.^{25–27} Other benefits of one-pot MCRs over multistep syntheses include their short reaction time and high chemical yields, which also leads to reduced waste generation, manpower, and energy consumption. Hence, MCRs have become a very powerful tool in combinational chemistry and drug discovery for the synthesis of biologically important heterocyclic compounds.

N-Heterocyclic scaffolds are very common in naturally occurring compounds. Among the heterocyclic compounds, the 2-amino-3,5-dicarbonitrile-6-thio-pyridines ring system has attracted much attention due to its widespread occurrence in numerous bioactive natural products. Such compounds have enjoyed wide applications in diverse pharmacological activities, such as anti-bacterial,²⁸ anti-prion,²⁹ anticancer agents,³⁰ and anti-hepatitis B virus.³¹ (Scheme 1).

Furthermore, they can act as potassium channel openers for the treatment of urinary incontinence. In addition, some of these compounds were discovered to be candidates for the development of new drugs for the treatment of cancer, Parkinson's disease, epilepsy, hypoxia/ischemia, kidney disease, and asthma.³² For example, there are some naturally occurring compounds **I**, **II**, and **III** that bear a pyridine group as a structural subunit,^{33–35} while compounds **IV** and **V** are commercially available drug molecules that have the pyridine skeleton (Scheme 2).³⁶

Diverse approaches have been developed for preparing pyridine derivatives with multistep methods.^{37–39} Recently, the reaction between aldehyde, malononitrile, and thiol *via* a one-pot pseudo-four component reaction was evaluated as an efficient and simple method for the preparation of 2-amino-3,5-dicarbonitrile-6-thio-pyridines in the presence of a catalyst. In recent years, more effective catalysts for the preparation of pyridine derivatives have been reported, such as ZnCl₂,⁴⁰ NAP-MgO,⁴¹ iodoxybenzoic acid (IBX),⁴² DBU,⁴³ KF/alumina,⁴⁴ scandium(III) triflate,⁴⁵ [bmIm]OH,⁴⁶ DABCO,⁴⁷ WEB,⁴⁸ Fe₂O₃@Fe₃O₄@Co₃O₄,⁴⁹ NaNH₂,⁵⁰ Cu(I) nanoparticles,⁵¹ Zn(II) and Cd(II) MOFs,⁵² microporous molecular sieves 4A,⁵³ and phosphotungstic acid/CTAB.⁵⁴ Nevertheless, some previously reported procedures remain valuable, albeit many of these procedures have significant drawbacks, such as low yields, tedious workup procedures, high temperatures, long reaction times, and the use of phosphine ligands and copper salts. For example, Evodkimov *et al.* developed a new method for the synthesis of pyridines

derivatives using DABCO or Et₃N as a base catalyst. One of the limitations of that method was that the corresponding products were obtained in yields of only 20–48%.⁴⁷ Sridhar *et al.* reported a new ZnCl₂ as a Lewis acid catalyst for the synthesis of pyridines derivatives under exotic reaction conditions (conventional heating or microwave heating). The ZnCl₂ catalyst gave the products in 45–73% and 46–67% yields, respectively.⁴⁰ It was further observed that some methods used expensive or toxic catalysts and reagents.⁴³ Therefore, the development of an environmentally friendly and green route for the synthesis of pyridine derivatives is still a desirable goal.

Continuing our endeavors for preparing and designing new magnetic nanoparticles as nanocatalysts,^{55–58} herein, for the first time, we report the synthesis of Ni^{II}-picolylamine/TCT/APTES@SiO₂@Fe₃O₄ as a heterogeneous nanocatalyst. This catalyst could be successfully used in the one-pot pseudo-four component synthesis of substituted pyridine derivatives (Scheme 3).

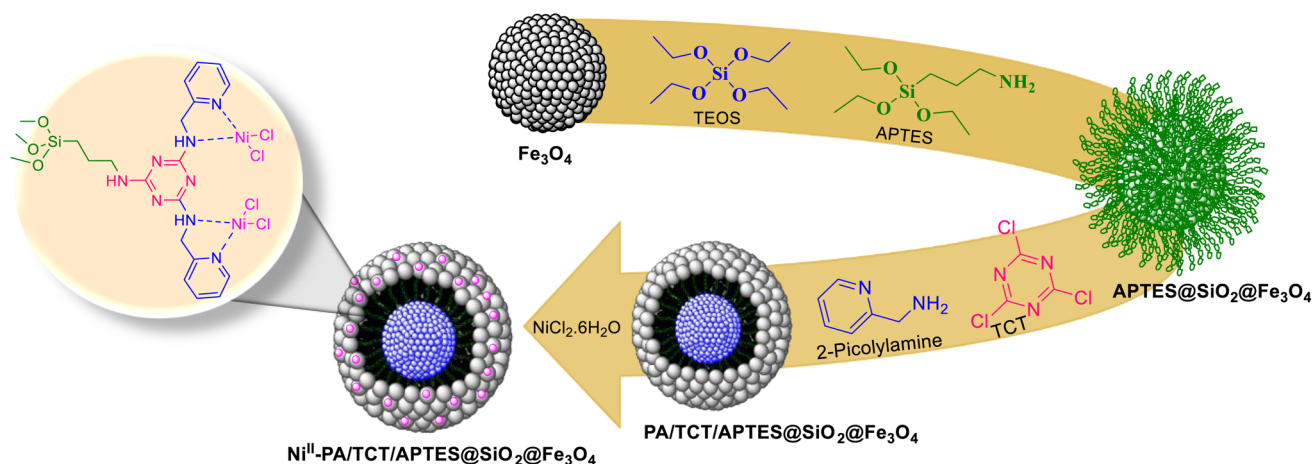
Results and discussion

Preparation of Ni^{II}-picolylamine/TCT/APTES@SiO₂@Fe₃O₄

Ni^{II}-picolylamine/TCT/APTES@SiO₂@Fe₃O₄ was made according to a convenient and simple four-step operation process, as illustrated in Scheme 4. Silica-coated Fe₃O₄ was initially obtained by attaching Fe₃O₄ to tetraethyl orthosilicate. In the next step, the resulting Fe₃O₄@SiO₂ was coated with (3-aminopropyl) triethoxysilane (APTES), followed by treatment with 2,4,6-trichloro-1,3,5-triazine (TCT) as a cross-linking agent in THF at room temperature. The chloride atoms in the cyanuric chloride agent were alternatively substituted to amine groups in APTES and 2-picolylamine at diverse temperatures, respectively. Picolylamine/TCT/APTES@SiO₂@Fe₃O₄ was formed through the reaction between Fe₃O₄@SiO₂@NH₂@TCT and 2-picolylamine under reflux conditions in CH₃CN. Finally, the reaction with a solution of nickel(II) chloride hexahydrate and picolylamine/TCT/APTES@SiO₂@Fe₃O₄ in EtOH at room temperature gave Ni^{II}-picolylamine/TCT/APTES@SiO₂@Fe₃O₄ (Scheme 4).

Characterization of Ni^{II}-picolylamine/TCT/APTES@SiO₂@Fe₃O₄ catalyst

The as-prepared nanocatalyst was characterized using various techniques, including FT-IR, XPS, TGA, VSM, TEM, XRD, BET,



Scheme 4 Preparation of the Ni^{II}-picolylamine/TCT/APTES@SiO₂@Fe₃O₄ catalyst.

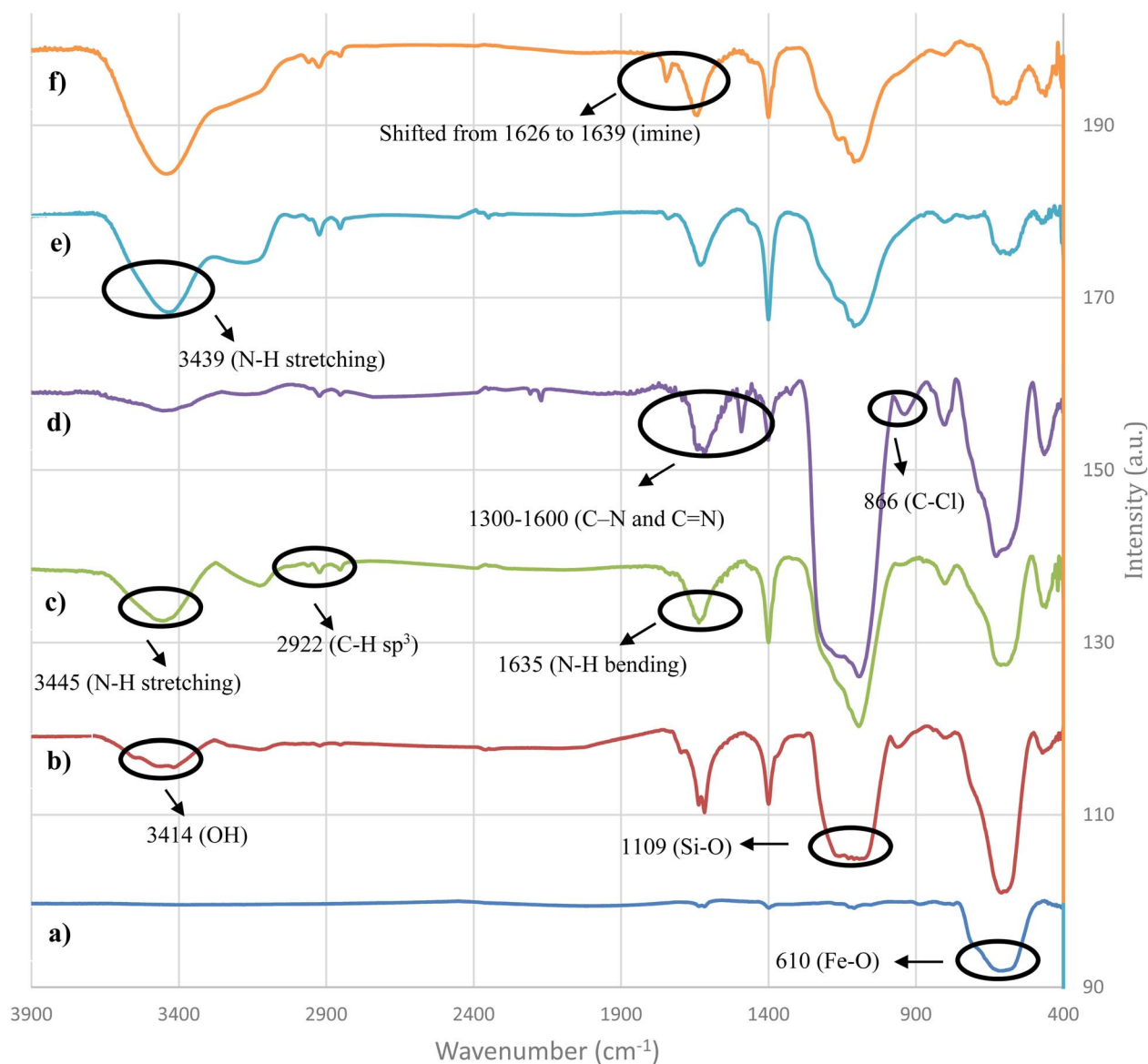


Fig. 1 FT-IR spectra of (a) Fe₃O₄, (b) SiO₂@Fe₃O₄, (c) APTES@SiO₂@Fe₃O₄, (d) TCT/APTES@SiO₂@Fe₃O₄, (e) picolylamine/TCT/APTES@SiO₂@Fe₃O₄, and (f) Ni^{II}-picolylamine/TCT/APTES@SiO₂@Fe₃O₄.



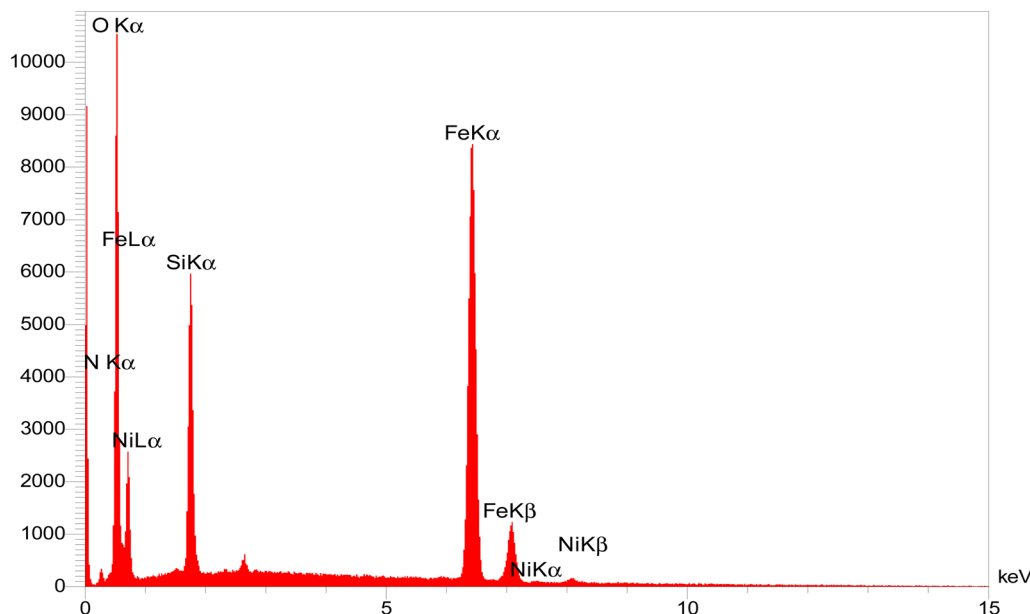


Fig. 2 EDX spectrum of Ni^{II} -picolylamine/TCT/APTES@ SiO_2 @ Fe_3O_4 catalyst.

FE-SEM, ICP, and EDX. FT-IR spectra were obtained for assessing the chemical changes during the synthesis of the Ni^{II} -picolylamine/TCT/APTES@ SiO_2 @ Fe_3O_4 catalyst in the range of 400 to 3900 cm^{-1} , and the results are displayed in Fig. 1. As can be seen in the FT-IR spectrum of pure magnetic nanoparticles, the strong absorption at 610 cm^{-1} was associated with the Fe–O bond, and confirmed the synthesis of iron oxide (Fig. 1a).^{57,58} Two absorption peaks at 1109 and 3414 cm^{-1} were observed, attributed to the presence of Si–O–Si and OH groups, respectively (Fig. 1b).^{57,58} After immobilizing APTES on the silica-coated Fe_3O_4 , new bands appeared at 3445 and 1635 cm^{-1} , which were assigned to N–H stretching vibration and N–H bending vibration of NH_2 , respectively. Furthermore, the new band detected at 2922 cm^{-1} was due to the C–H(sp^3) of a $-\text{CH}_2$ group, indicating the APTES coating on the SiO_2 @ Fe_3O_4 (Fig. 1c).^{57,58} The absorption peaks about 1300–1600 cm^{-1} in the TCT/APTES@ SiO_2 @ Fe_3O_4 spectra were associated with the C–N and C=N stretching vibrations, proving the TCT presence on the TCT/APTES@ SiO_2 @ Fe_3O_4 structure. Besides, the absorption band at 866 cm^{-1} was related to the unreacted C–Cl bond (Fig. 1d).^{57,58} After the reaction between TCT/APTES@ SiO_2 @ Fe_3O_4 with 2-picolylamine to give picolylamine/TCT/APTES@ SiO_2 @ Fe_3O_4 , as expected, the absorption peak for C–Cl disappeared (Fig. 1e). After the coordination of the $\text{Ni}(\text{II})$ metal ion, the imine peak shifted from 1626 to 1639 cm^{-1} . These obtained result indicated the coordination of $\text{Ni}(\text{II})$ metal ion on the surface of picolylamine/TCT/APTES@ SiO_2 @ Fe_3O_4 (Fig. 1f).^{57,58}

EDX spectroscopy is one of the most significant elemental analyses to chemically characterize samples with high accuracy. The EDX spectrum clearly showed the presence of O, Fe, Si, C, N, and Ni elements in the catalyst with mass percentages of 36.0, 39.0, 19.71, 2.83, 1.45, and 1.01, respectively, indicating the catalyst had been successfully prepared. The Ni loading onto

the Ni^{II} -picolylamine/TCT/APTES@ SiO_2 @ Fe_3O_4 catalyst was confirmed by the peak presence of the Ni element in the EDX spectrum (Fig. 2). Moreover, ICP was used to confirm the exact amount of Ni loading of the catalyst. The ICP results clearly showed the presence of Ni (1.77%) in the catalyst.

Further, the presence of O, Fe, Si, C, N, and Ni elements in the Ni^{II} -picolylamine/TCT/APTES@ SiO_2 @ Fe_3O_4 catalyst was confirmed by another elemental analysis, namely elemental mapping analysis (Fig. 3). Fig. 3 clearly indicates the presence of O, Fe, Si, C, N, and Ni elements in the catalyst with a suitable dispersity. Moreover, the results from the elemental mapping analysis confirmed the EDX analysis.

XPS was performed from 0 to 1200 eV for the Ni^{II} -picolylamine/TCT/APTES@ SiO_2 @ Fe_3O_4 catalyst to obtain the oxidation of the Ni state together with elemental analysis (Fig. 4). Fig. 4a–f illustrate the spectra for (a) Fe 2p, (b) C 1s, (c) N 1s, (d) Ni 2p, (e) Si 2p, and (f) O 1s elements in Ni^{II} -picolylamine/TCT/APTES@ SiO_2 @ Fe_3O_4 . Fig. 4a demonstrates the high-resolution spectra of Fe 2p with two peaks at 712.6 and 726.4 eV, attributed to $2\text{p}_{3/2}$ and $2\text{p}_{1/2}$, respectively.⁵⁸ The peaks at binding energies of 283.8 and 286.4 eV were attributed to C–C and C–O, respectively (Fig. 4b).⁵⁸ Fig. 4c depicts the high-resolution spectrum of N 1s with two peaks at 401.2 and 404.6 eV related to C–N and C=N, respectively.⁵⁸ The XPS spectrum for Ni showed doublet peaks at 855.8 and 864.9 eV related to $\text{Ni } 2\text{p}_{3/2}$ and $\text{Ni } 2\text{p}_{1/2}$, respectively (Fig. 4d).^{59,60} These peaks well confirmed the oxidation state of $\text{Ni}(\text{II})$ in the catalyst. The Si 2p appear at ≈ 102.7 eV and 104.8 eV, respectively related to the Si–C and Si–O, respectively (Fig. 4e).⁵⁸ Finally, Fig. 4f reveals the O atoms contained in as-prepared nanocatalyst. O 1s at 530.2 eV, 534.8 eV and 535.2 eV corresponding to Fe–O, Si–O and O–H, respectively.⁵⁸

The crystalline structure of Ni^{II} -picolylamine/TCT/APTES@ SiO_2 @ Fe_3O_4 was investigated by powder X-ray



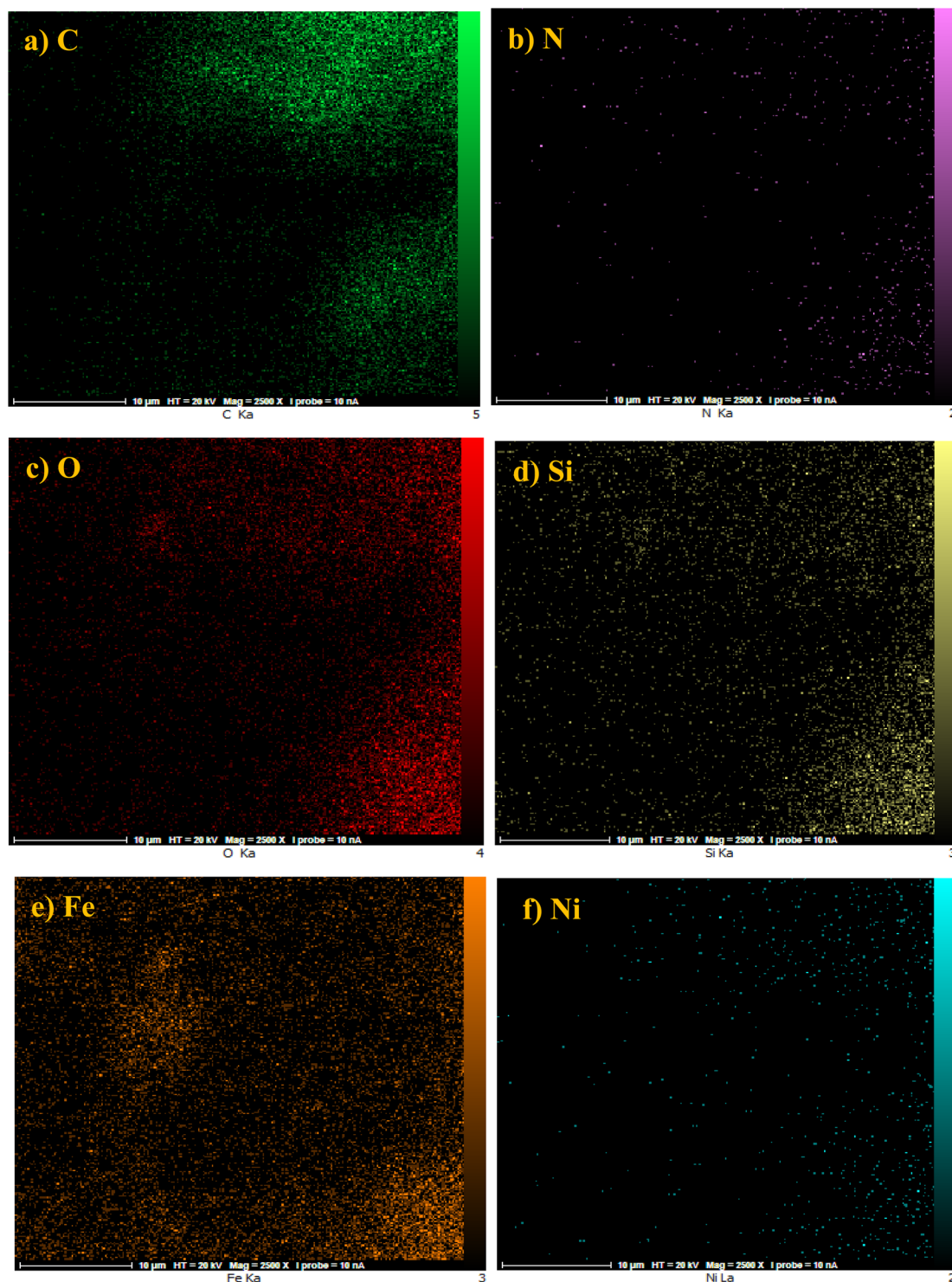


Fig. 3 Elemental mapping analysis of Ni^{II} -picolylamine/TCT/APTES@ SiO_2 @ Fe_3O_4 catalyst: (a) C, (b) N, (c) O, (d) Si, (e) Fe, and (f) Ni.

diffraction (PXRD) (Fig. 5). Fig. 5 displays strong and sharp peaks at $2\theta = 30.45^\circ$, 35.44° , 35.68° , 43.24° , 53.69° , 57.14° , and 62.86° belonging to Ni^{II} -picolylamine/TCT/APTES@ SiO_2 @ Fe_3O_4 which was well consistent with the Fe_3O_4 nanoparticle crystal structure. Besides, the obtained result demonstrated that the designed catalyst had been successfully synthesized and there was no damage to the crystalline structure of Fe_3O_4 , and the

crystallographic faces were in good agreement with the XRD pattern of cubic Fe_3O_4 NP (JCPDS 88-0866).^{57,58} The crystallite average size and interplanar distance of the catalyst were determined to be 28.7 nm and 0.208 nm from the XRD spectra according to FWHM calculations using the Scherrer formula and Bragg equation, respectively (Table S1, ESI†).



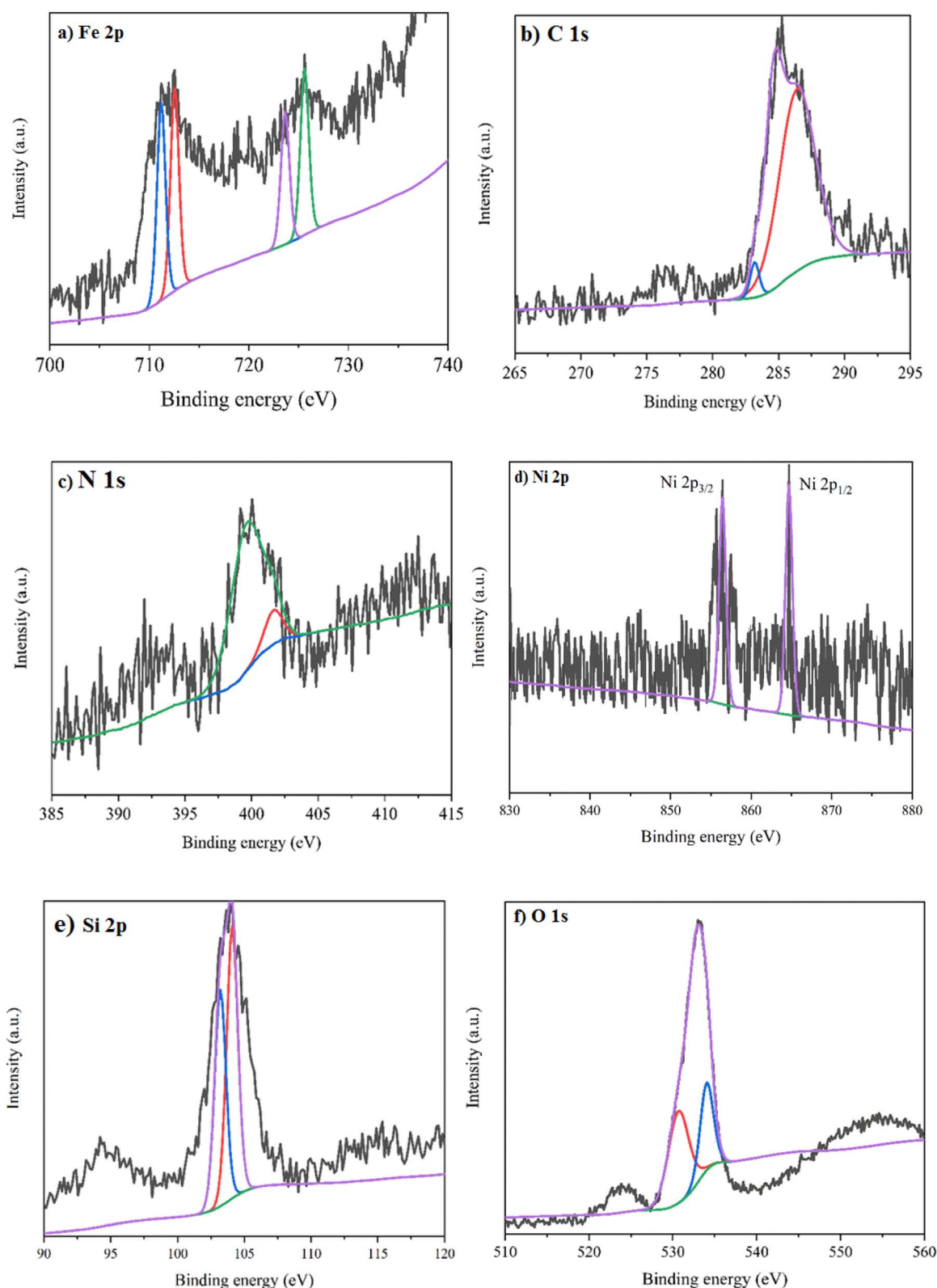


Fig. 4 XPS spectra of Ni^{II} -picolylamine/TCT/APTES@ SiO_2 @ Fe_3O_4 catalyst: (a) Fe 2p, (b) C 1s, (c) N 1s, (d) Ni 2p, (e) Si 2p, and (f) O 1s.

The magnetic properties of Fe_3O_4 and Ni^{II} -picolylamine/TCT/APTES@ SiO_2 @ Fe_3O_4 were studied at ambient temperature by VSM analysis (Fig. 6). Fig. 6a clearly indicates that these

nanoparticles of (a) Fe_3O_4 and (b) Ni^{II} -picolylamine/TCT/APTES@ SiO_2 @ Fe_3O_4 had a superparamagnetic nature. The magnetic saturation value for pure Fe_3O_4 was observed at 58.74

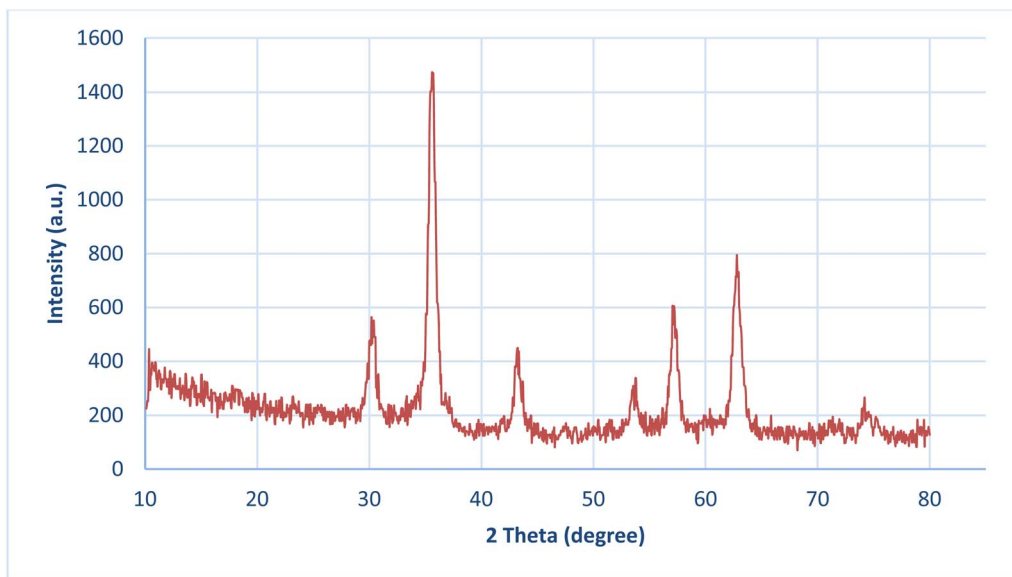


Fig. 5 XRD patterns of Ni^{II} -picolylamine/TCT/APTES@ SiO_2 @ Fe_3O_4 catalyst.

emu g^{-1} . After coating various organic compounds on the surface of pure Fe_3O_4 to synthesize the Ni^{II} -picolylamine/TCT/APTES@ SiO_2 @ Fe_3O_4 , the magnetic saturation value was observed at 37.02 emu g^{-1} . Nevertheless, this magnetic saturation value was sufficient for the catalyst's easy separation from the reaction mixture by employing a magnetic bar (Fig. 6b).

The thermal stability of Fe_3O_4 , SiO_2 @ Fe_3O_4 , and Ni^{II} -picolylamine/TCT/APTES@ SiO_2 @ Fe_3O_4 were investigated through TGA analysis in the temperature range of 25–600 °C (Fig. 7). Both the TGA diagram of Fe_3O_4 and silica-coated SiO_2 indicated a small weight loss below 100 °C, probably due to the removal of surface hydroxyl groups and physically adsorbed and trapped water molecules. For Ni^{II} -picolylamine/TCT/APTES@ SiO_2 @ Fe_3O_4 , there were two mass reductions: (i) below 100 °C, probably due to the evaporation of surface hydroxyl groups and physically adsorbed and trapped water molecules in the structure of the catalyst and (ii) between 180–600 °C, which was the main weight loss and probably due to the thermal decomposition of the functional groups and organic compounds supported on the catalyst surface. This thermal decomposition indicated the coating of various organic compounds on the iron oxide support. Moreover, the complete decomposition of the as-prepared nanocatalyst happened at about 500 °C.

The structural features, morphologies, and particle sizes of Fe_3O_4 and Ni^{II} -picolylamine/TCT/APTES@ SiO_2 @ Fe_3O_4 were investigated by FE-SEM, TEM, and size-distributions images (Fig. 8). The FE-SEM images indicated that Fe_3O_4 and Ni^{II} -picolylamine/TCT/APTES@ SiO_2 @ Fe_3O_4 had been synthesized with spherical shapes with the particle sizes in the 20–33 nm and of 31–42 nm ranges, respectively (Fig. 8a and b). In another study, the uniformity and morphology of Fe_3O_4 and Ni^{II} -picolylamine/TCT/APTES@ SiO_2 @ Fe_3O_4 were further investigated by TEM (Fig. 8c and d). Fig. 8d clearly indicates that the particles had been synthesized with a uniform size and core/shell. Further, the size distribution of the Ni^{II} -picolylamine/TCT/

APTES@ SiO_2 @ Fe_3O_4 was measured by TEM to be over 28 nm, which suitably matched with the results obtained from the XRD analysis (Fig. 8e).

The isotherm type, total pore volume, mean pore diameter, and surface area of Ni^{II} -picolylamine/TCT/APTES@ SiO_2 @ Fe_3O_4 were determined by BET analysis (Fig. 9). As can be seen from Fig. 9a, the structure of the as-prepared nanocatalyst could be ascribed to the type IV isotherm with a distinct hysteresis loop indicating mesoporous structure.^{57,58} Fig. 9b shows that the as-prepared nanocatalyst sat in the P/P_0 range of 0.006–0.007 with a strong inflection, which may have been because the capillary condensation of N_2 was reflected in the mesopores. Further, the corresponding structural parameters of the as-prepared nanocatalyst included a total pore volume, mean pore diameter, and surface area of $0.189 \text{ cm}^3 \text{ g}^{-1}$, 22.31 nm, and $53.61 \text{ m}^2 \text{ g}^{-1}$, respectively.

Catalytic activity test

Activity tests for the prepared Ni^{II} -picolylamine/TCT/APTES@ SiO_2 @ Fe_3O_4 catalyst were performed for the one-pot synthesis of substituted pyridine derivatives. For this, a one-pot pseudo-four component reaction of malononitrile (2 mmol), thiophenol (1 mmol), and benzaldehyde (1 mmol) was tested initially as a model reaction for the synthesis of **4a**. In this study, we investigated the effect of various solvents, loadings of catalyst, and temperatures, and the obtained results are summarized in Table 1. When the reaction was stirred in the absence of the as-prepared nanocatalyst under solvent-free conditions at room temperature, a trace amount of **4a** was obtained even after 24 h (Table 1, entry 1). Similarly, when the reaction was stirred under the same condition at 80 °C, only a trace amount of **4a** was obtained even after 24 h (Table 1, entry 2). It was observed that in the presence of the catalyst, the product was indeed obtained. Initially, we tried the reaction with 0.005 g of the as-prepared



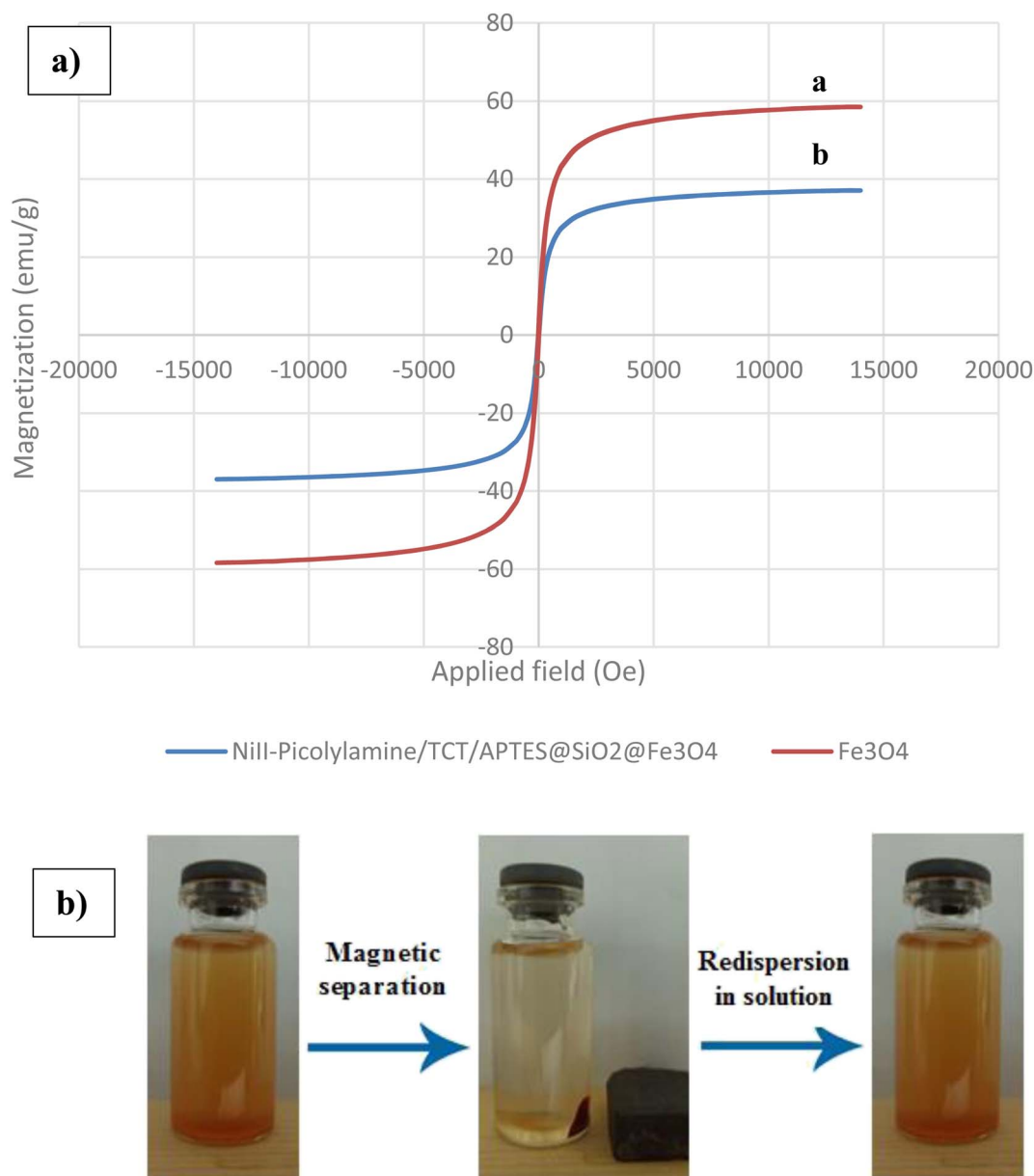


Fig. 6 (a) VSM analysis, (b) image of the magnetic separation and redispersion of Ni^{II}-picolylamine/TCT/APTES@SiO₂@Fe₃O₄.

nanocatalyst under solvent-free conditions at 80 °C and a yield of 43% of **4a** was obtained (Table 1, entry 3). When the catalyst loading was increased to 0.01 g and 0.03 g under the same conditions, 62% and 75% yields of **4a** were obtained (Table 1, entries 4 and 5). The best result was obtained when the reaction was carried out with 0.05 g of the as-prepared nanocatalyst under solvent-free conditions, whereby the reaction yield increases to 95% after 30 min (Table 1, entry 6). On increasing the amount of catalyst to 0.07–0.1 g of the as-prepared nanocatalyst, 95%, 93%, and 91% product yields were obtained, respectively (Table 1, entries 7–9). In the next study, we examined the effect of various solvents, such as MeOH, H₂O, CH₂Cl₂, CHCl₃, H₂O : EtOH (1 : 1), EtOH, and EG on the reaction. The obtained results indicated the products were obtained in moderate yield (Table 1, entries 10–14).

In EtOH produced a 92% product yield after 60 min (Table 1, entry 15). The screening of various solvents indicated that the EG as the solvent was more effective than the other solvents. In addition, in the solvent-free condition, when the reaction was performed by EG in the presence of 0.05 g of as-prepared nanocatalyst under reflux conditions, 96% product was obtained after 35 min (Table 1, entry 16).

In the next study, we investigated the one-pot pseudo-four component reaction of malononitrile (2 mmol), thiophenol (1 mmol), and benzaldehyde (1 mmol), using various catalysts, such as Fe₃O₄, SiO₂@Fe₃O₄, APTES@SiO₂@Fe₃O₄, TCT/APTES@SiO₂@Fe₃O₄, picolylamine/TCT/APTES@SiO₂@Fe₃O₄, and NiCl₂·6H₂O for the synthesis of **4a** under solvent-free conditions at 80 °C, and the results are listed in Table 2. As

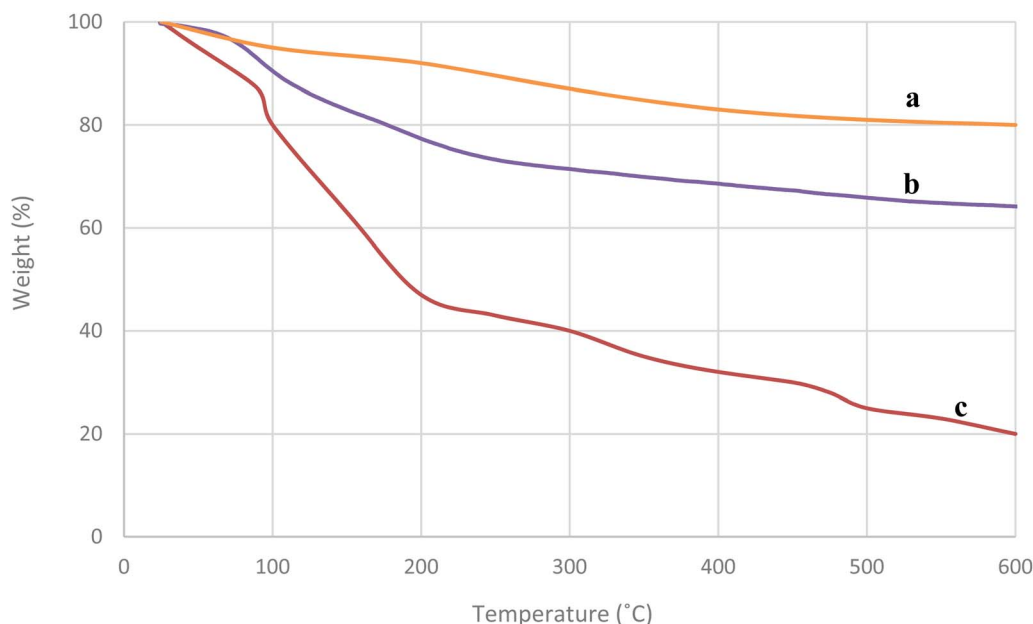


Fig. 7 TGA analysis of (a) Fe₃O₄, (b) SiO₂@Fe₃O₄, and (c) Ni^{II}-picolylamine/TCT/APTES@SiO₂@Fe₃O₄.

can be seen, it was found that Ni^{II}-picolylamine/TCT/APTES@SiO₂@Fe₃O₄ catalyze the reaction with high yield and short reaction time than the other catalysts.

Knowing the optimized conditions (using 0.05 g of the as-prepared nanocatalyst under solvent-free conditions or EG at 80 °C), a range of aromatic aldehydes containing electron-withdrawing and electron-donating groups were reacted with malononitrile and thiophenol, and afforded the corresponding products (**4a–l**), and good results were obtained (Table 3). In method A, Ni^{II}-picolylamine/TCT/APTES@SiO₂@Fe₃O₄ as a high-performance heterogeneous nanocatalyst was used for the reaction of malononitrile, thiophenol, and various aldehydes under solvent-free conditions at 80 °C and gave satisfactory yields (91–97%) after 10–55 min. Moreover, Ni^{II}-picolylamine/TCT/APTES@SiO₂@Fe₃O₄ as a high-performance heterogeneous nanocatalyst showed excellent activity for the reaction of malononitrile, thiophenol, and various aldehydes in EG at 80 °C. The corresponding products were furnished in short reaction times (8–45 min) and in excellent yields (89–97%). Generally, Ni^{II}-picolylamine/TCT/APTES@SiO₂@Fe₃O₄ displayed remarkable efficiency for the one-pot synthesis of substituted pyridine derivatives in both methods A and B.

Due to environmental concerns, the catalyst reusability was tested (Fig. 10). For this, we carried out the reaction between 4-nitrobenzaldehyde (1 mmol), malononitrile (2 mmol), and thiophenol (1 mmol) in the presence of Ni^{II}-picolylamine/TCT/APTES@SiO₂@Fe₃O₄ in EG at 80 °C. After the reaction completion, the catalyst could be separated easily from the reaction mixture by using a simple magnet. Then, the recovered catalyst was washed with EtOH (3 × 10 mL) and dried at room temperature for reused in the next run. This catalyst was reused up to eight times with only a slight decrease in activity, whereby the yields from the reaction smoothly decreased from 97% to

87% during 25–33 min (Fig. 10a). This slight decrease in the catalytic activity of the recovered nanocatalyst was due to the small leaching of Ni (1%) in the reaction after eight runs. The nanocatalyst was investigated by various analyses, including TEM and size distribution after each run for eight times. The TEM image was obtained for the recovered nanocatalyst after the eight runs (Fig. 10b), and indicated that the recovered nanocatalyst had a nearly uniform size and spherical shape, similar to the fresh catalyst. Likewise, the size distribution of the recovered nanocatalyst was measured by TEM, and was nearly same as the fresh catalyst (Fig. 10c).

In another study, the effect of leaching of the active species in the reaction mixture on the stability of the as-prepared nanocatalyst was investigated. To address this possibility, we used ICP-AES analysis of the fresh state of the catalyst and also the recovered catalyst after eight runs. The reaction on the basis of ICP-AES analysis showed a leaching of Ni of 1 wt% after the eight runs. This result obtained could explain the negligible decrease in the yield of the product **4b** with the increased recycling.

Large-scale synthesis of the reaction between 4-nitrobenzaldehyde (7 mmol, 1.05 g), malononitrile (14 mmol, 0.92 g), and thiophenol (7 mmol, 0.77 g) was performed in the presence of Ni^{II}-picolylamine/TCT/APTES@SiO₂@Fe₃O₄ in EG (21 mL) at 80 °C to give the corresponding **4b** to prove the scalability and the prospective use of the current method (Scheme 5). The obtained results indicated that when performing the large-scale synthesis, the desired product was obtained with an 89% yield.

A plausible mechanism for obtaining the substituted pyridine derivatives in the reaction catalyzed by Ni^{II}-picolylamine/TCT/APTES@SiO₂@Fe₃O₄ is indicated in Scheme 6. The reaction was accelerated *via* the surface properties, including by Ni²⁺ acting as a Lewis acid. Initially, the Lewis acid site of the as-



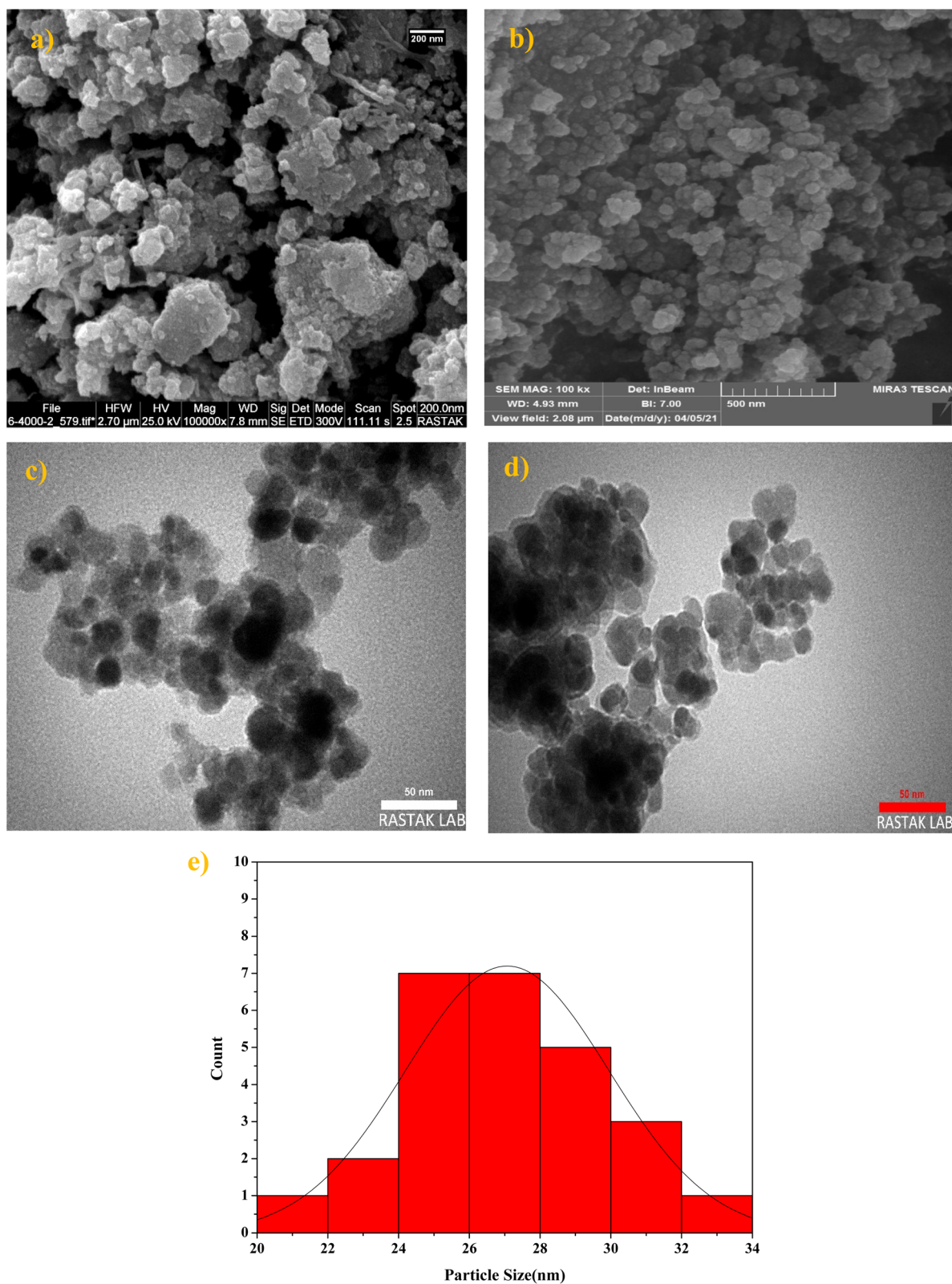


Fig. 8 FE-SEM of (a) Fe_3O_4 , (b) Ni^{II} -picolylamine/TCT/APTES@ SiO_2 @ Fe_3O_4 . TEM of (c) Fe_3O_4 , (d) Ni^{II} -picolylamine/TCT/APTES@ SiO_2 @ Fe_3O_4 , and (e) size distribution of Ni^{II} -picolylamine/TCT/APTES@ SiO_2 @ Fe_3O_4 .

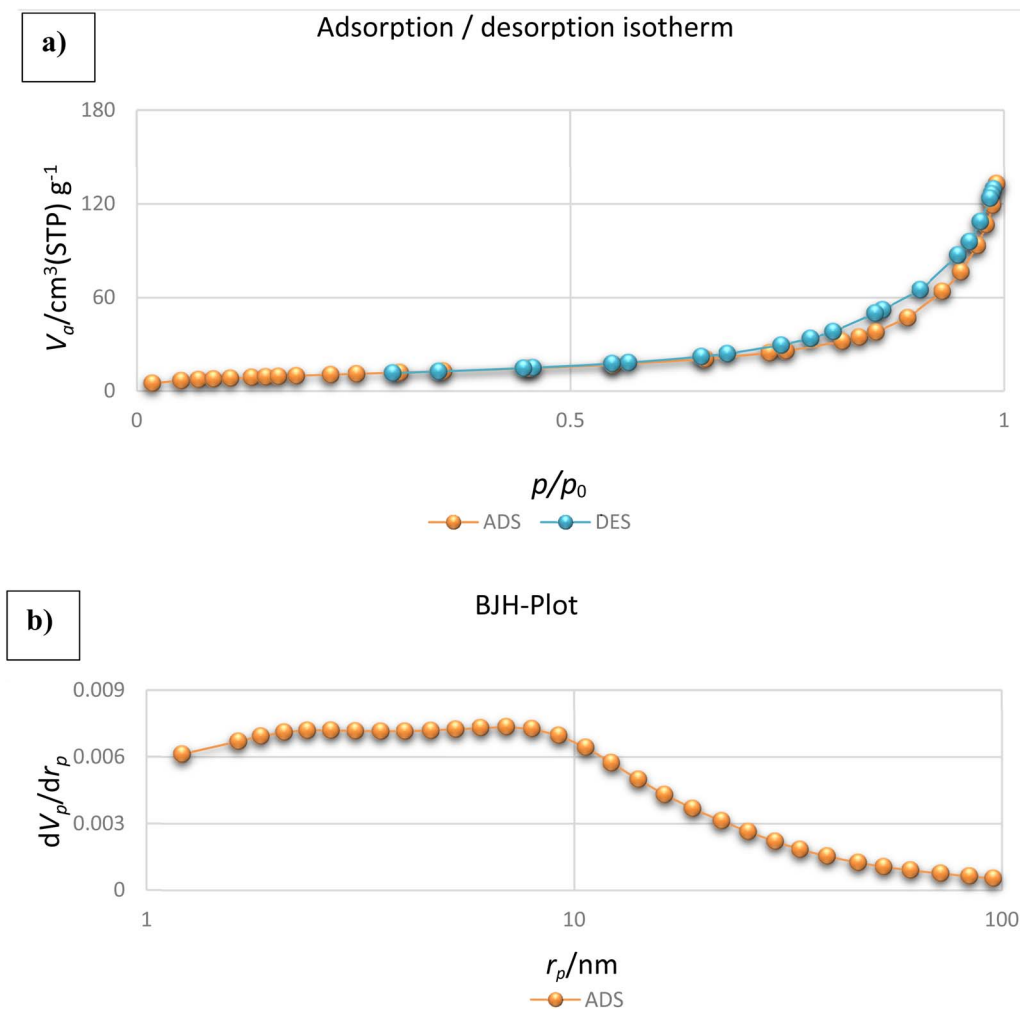


Fig. 9 (a) BET plot of the nitrogen adsorption–desorption and (b) pore-size distribution curve of the Ni^{II} -picolylamine/TCT/APTES@ SiO_2 @ Fe_3O_4 .

prepared nanocatalyst activated the aldehyde **A** and malononitrile **B**, and produced the 2-arylidene malononitrile **C** via a Knoevenagel condensation. In the next step, Ni^{2+} catalyzed the thiophenol **D** and malononitrile **B** and via a Michael addition to the intermediate **C** led to producing the intermediate **F**. Then, dihydropyridine **G** was formed via the tautomerization of the Michael product **F**, followed by yielding the desired product **H**.

Experimental

Materials and methods

All of the used materials were purchased from Fluka (Switzerland), Sigma-Aldrich, and Merck (Germany): iron(III) chloride, 25% ammonia, $\text{FeSO}_4 \cdot 7\text{H}_2\text{O}$, (3-aminopropyl)triethoxysilane, ethanol, tetraethyl orthosilicate, cyanuric chloride, tetrahydrofuran, 2-picolylamine, $\text{NiCl}_2 \cdot 6\text{H}_2\text{O}$, malononitrile, various aromatic aldehydes, and thiophenol. ^1H and ^{13}C NMR spectra were obtained applying CDCl_3 or $\text{DMSO}-d_6$ solvent on a Bruker DRX-250 AVANCE spectrometer (at 250 and 62.5 MHz). FT-IR spectra were acquired by employing a PerkinElmer 597 spectrophotometer. The EDAX spectra were applied for the

elemental analysis of Ni^{II} -picolylamine/TCT/APTES@ SiO_2 @ Fe_3O_4 . PXRD analysis was performed on an X'Pert-PRO advanced diffractometer operated at 40 kV and 40 mA at r.t to investigate the crystalline structure of the synthesized catalyst. The surface atomic concentration and chemical composition of Ni^{II} -picolylamine/TCT/APTES@ SiO_2 @ Fe_3O_4 were investigated using XPS at an energy of 1253.6 eV (Esfahan University, Esfahan, Iran). SEM analysis was recorded on a TE-SCAN system (Brno, Czech Republic). TEM images were recorded using a Zeiss EM10C microscope operating at 80 kV. VSM analysis was applied to verify the magnetic properties of Ni^{II} -picolylamine/TCT/APTES@ SiO_2 @ Fe_3O_4 (VSM, Taban, Tehran, Iran).

Fe_3O_4 synthesis

The coprecipitation procedure was applied for the preparation of magnetic Fe_3O_4 . First, 0.9 g of $\text{FeSO}_4 \cdot 7\text{H}_2\text{O}$ with 0.97 g of FeCl_3 in 120 mL of deionized H_2O were dissolved at 80 °C under a N_2 gas atmosphere, and then a 25% aqueous ammonia solution (120 mL, 1.5 M) was added dropwise into the solution under stirring. In the following, the obtained black mixture was stirred under N_2 gas for 30 min. The reaction mixture was cooled to 25 °C, and the



Table 1 Combined effects of the catalyst loading, temperature, and solvents for the synthesis of **4a**^a

Entry	Catalyst (g)	Solvent (3 mL)	Temperature (°C)	Time (min)	Yield ^b (%)
1	None	Solvent-free	Room temperature	24 (h)	Trace
2	None	Solvent-free	80	24 (h)	Trace
3	0.005	Solvent-free	80	130	43
4	0.01	Solvent-free	80	90	62
5	0.03	Solvent-free	80	60	75
6	0.05	Solvent-free	80	30	95
7	0.07	Solvent-free	80	35	95
8	0.09	Solvent-free	80	40	93
9	0.1	Solvent-free	80	40	91
10	0.05	MeOH	Reflux	120	45
11	0.05	H ₂ O	Reflux	90	78
12	0.05	CH ₂ Cl ₂	Reflux	180	51
13	0.05	CHCl ₃	Reflux	180	44
14	0.05	H ₂ O : EtOH (1 : 1)	80	60	83
15	0.05	EtOH	Reflux	60	92
16	0.05	EG	80	20	96

^a Reaction conditions: malononitrile (2 mmol), thiophenol (1 mmol), benzaldehyde (1 mmol), catalyst, and solvent (3 mL). ^b Isolated yield.**Table 2** Effects of various catalyst for the synthesis of **4a**^a

Entry	Catalyst	Time (h)	Yield ^b (%)
1	Fe ₃ O ₄	4	41
2	SiO ₂ @Fe ₃ O ₄	3	55
3	APTES@SiO ₂ @Fe ₃ O ₄	1	71
4	TCT/APTES@SiO ₂ @Fe ₃ O ₄	24	10
5	Picolylamine/TCT/APTES@SiO ₂ @Fe ₃ O ₄	6	25
6	NiCl ₂ ·6H ₂ O	6	45
7	Ni ^{II} -picolylamine/TCT/APTES@SiO ₂ @Fe ₃ O ₄	30 min	95

^a Reaction conditions: malononitrile (2 mmol), thiophenol (1 mmol), benzaldehyde (1 mmol), and catalyst (0.05 g) under solvent-free conditions at 80 °C. ^b Isolated yield.

resulting black precipitate was isolated by applying a simple magnet and washed several times with deionized H₂O and EtOH, and dried at 40 °C for 24 h (yield: 92%).

Synthesis of SiO₂@Fe₃O₄

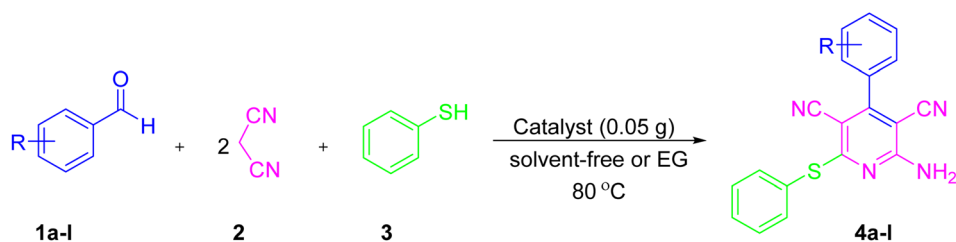
First, 1 g of Fe₃O₄ was dispersed in a mixture of EtOH : distilled H₂O (80 : 20; 100 mL) with applying sonification for 30 min.



Table 3 Ni^{II} -picolyamine/TCT/APTES@ SiO_2 @ Fe_3O_4 -catalyzed reaction of malononitrile, thiophenol, and various aldehydes under solvent-free conditions or EG at 80 °C

Entry	Product	Method A ^a % Yield ^c (reaction time)	Method B ^b % Yield ^c (reaction time)	Melting point (°C)
1	 4a	95 (30 min)	96 (20 min)	217–219 (ref. 51)
2	 4b	97 (15 min)	96 (10 min)	285–287 (ref. 51)
3	 4c	94 (35 min)	93 (30 min)	220–222 (ref. 51)
4	 4d	96 (10 min)	97 (8 min)	271–273 (ref. 51)
5	 4e	93 (50 min)	95 (40 min)	209–211 (ref. 51)





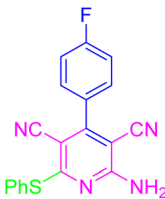
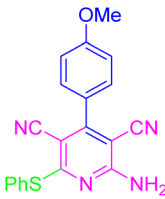
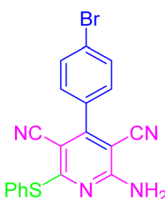
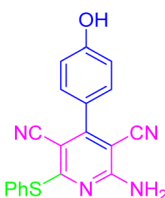
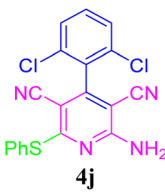
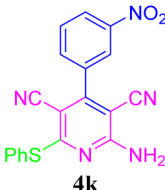
Entry	Product	Method A ^a	Method B ^b	Melting point (°C)
		% Yield ^c (reaction time)	% Yield ^c (reaction time)	
6	 4f	91 (30 min)	92 (25 min)	224–226 (ref. 53)
8	 4g	92 (50 min)	91 (40 min)	238–240 (ref. 51)
9	 4h	95 (35 min)	94 (30 min)	256–258 (ref. 51)
10	 4i	94 (55 min)	89 (45 min)	314–316 (ref. 51)
11	 4j	96 (30 min)	92 (25 min)	183–185 (ref. 51)
12	 4k	96 (20 min)	96 (15 min)	217–219 (ref. 51)

Table 3 (Contd.)

Entry	Product	Method A ^a % Yield ^c (reaction time)	Method B ^b % Yield ^c (reaction time)	Melting point (°C)
13	 4l	93 (20 min)	93 (10 min)	—

^a Reaction conditions: Malononitrile (2 mmol), thiophenol (1 mmol), various aldehydes (1 mmol), and Ni^{II}-picolylamine/TCT/APTES@SiO₂@Fe₃O₄ (0.05 g) under solvent-free conditions at 80 °C. ^b Reaction conditions: Malononitrile (2 mmol), thiophenol (1 mmol), various aldehydes (1 mmol), and Ni^{II}-picolylamine/TCT/APTES@SiO₂@Fe₃O₄ (0.05 g) in EG (3 mL) at 80 °C. ^c Isolated yield.

Then, 2 mL of NH₃ solution 25% and 2 mL of TEOS (tetraethyl orthosilicate) were added and the obtaining solution was stirred under N₂ for 12 h. Finally, the obtained products were collected by employing a simple magnet and washed five times with distilled H₂O and once with EtOH. Eventually, SiO₂@Fe₃O₄ was afforded and dried in an oven at 40 °C for 24 h.

Synthesis of APTES@SiO₂@Fe₃O₄

First, 1 g of SiO₂@Fe₃O₄ in 100 mL of EtOH was suspended under ultrasonic radiation for 30 min, and then 4 mL of APTES under a nitrogen gas atmosphere was added to the dispersed solid NPs at 35 °C. Next, 4 mL of distilled H₂O was added to increase the hydrolysis rate of APTES, and the combination was stirred for 12 h under reflux conditions. Finally, the resulting APTES@SiO₂@Fe₃O₄ was obtained by applying a simple magnet, washed with several runs of deionized H₂O and EtOH, and dried in a vacuum at ambient temperature for 24 h (yield: 91%).

Synthesis of TCT/APTES@SiO₂@Fe₃O₄

First, 0.79 g of APTES@SiO₂@Fe₃O₄ in 100 mL of dry THF was suspended, and then 0.35 g of TCT was added and the resulting mixture was stirred for 16 h at room temperature. The afforded catalyst was washed three times with EtOH and dried under vacuum at ambient temperature (yield: 90%).

Synthesis of PA/TCT/APTES@SiO₂@Fe₃O₄

First, 0.5 mL of 2-picolyamine was slowly added to 100 mL of the ethanolic solution of TCT/APTES@SiO₂@Fe₃O₄ (0.1 g), and then the obtained mixture was stirred at ambient temperature

for 24 h. The obtained PA/TCT/APTES@SiO₂@Fe₃O₄ was isolated magnetically and washed several times with EtOH and dried under vacuum.

Synthesis of Ni^{II}-picolylamine/TCT/APTES@SiO₂@Fe₃O₄

First, 1 g of PA/TCT/APTES@SiO₂@Fe₃O₄ in 100 mL of EtOH was suspended by employing sonication for 30 min. On the other hand, 2.5 mmol of NiCl₂·6H₂O in 10 mL of EtOH was dissolved under vigorous stirring at ambient temperature to obtain a blue solution. Then, the solution of NiCl₂·6H₂O in EtOH was quickly added to the synthesized picolylamine/TCT/APTES@SiO₂@Fe₃O₄, which was then stirred under reflux conditions for 48 h. The solvent was evaporated under vacuum, and the Ni^{II}-picolylamine/TCT/APTES@SiO₂@Fe₃O₄ was washed three times with EtOH and then dried in air at ambient temperature.

Synthesis of pyridine derivatives

A mixture of the as-prepared nanocatalyst (0.05 g), malononitrile (2 mmol), thiophenol (1 mmol), and a variety of aldehyde derivatives (1 mmol) under solvent-free conditions or EG (3 mL) was heated to 80 °C in an oil bath until reaction completion. To evaluate the progress of the reaction, the mixture was monitored by thin-layer chromatography (TLC). After completion of the reaction, ethanol (15 mL) was added to the contents of the reaction container and stirred for 5 min. To reuse the as-prepared nanocatalyst in the next run, it was conveniently recovered from the reaction mixture by employing a magnetic bar and washed three times with ethanol. The synthesized products were recrystallized from hot ethanol to afford the pure product.



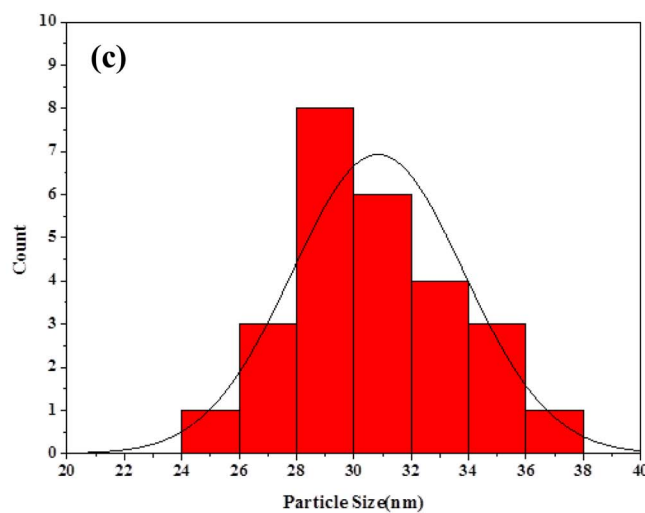
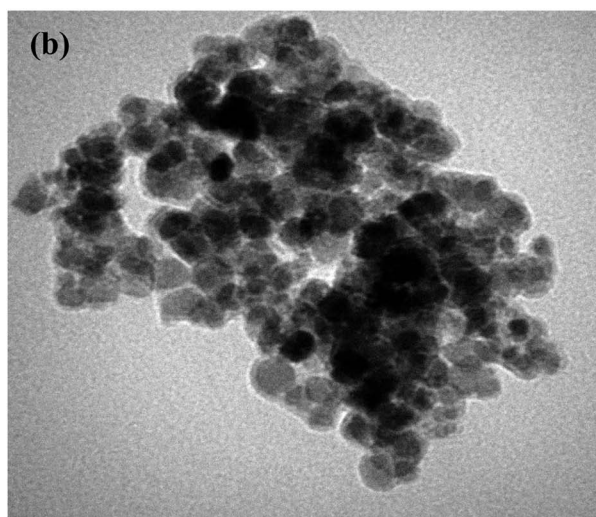
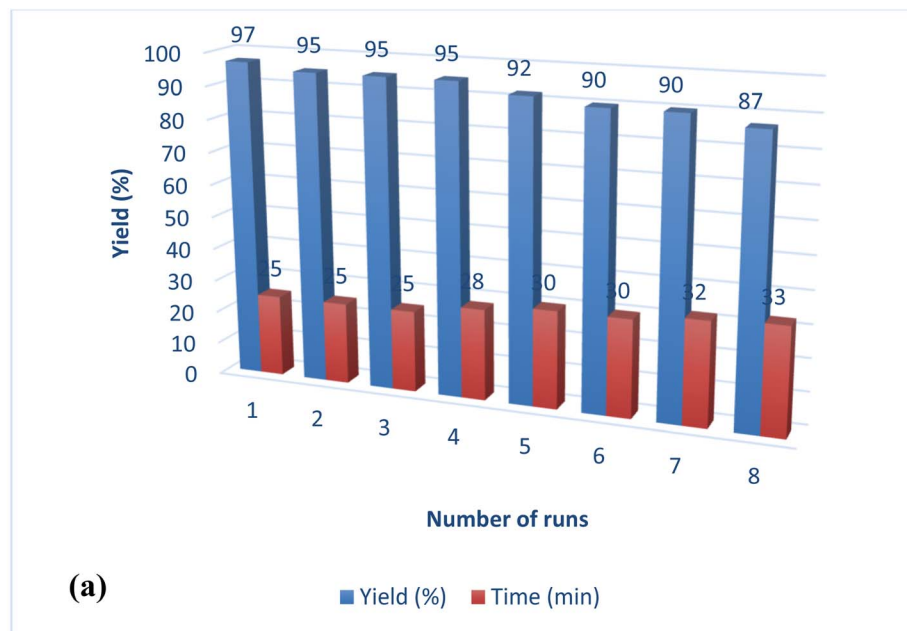
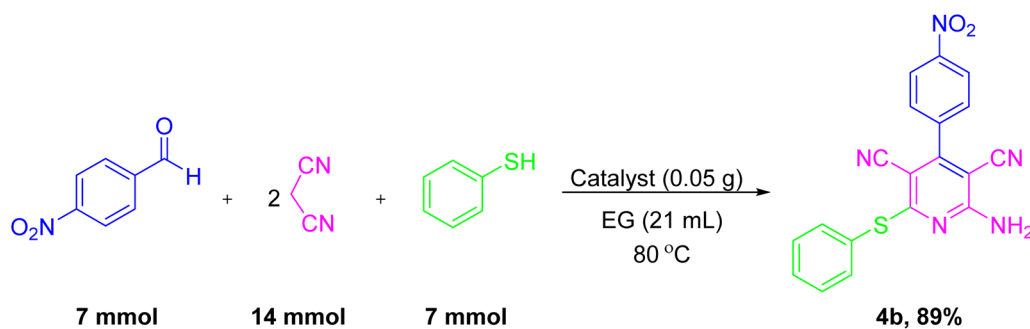
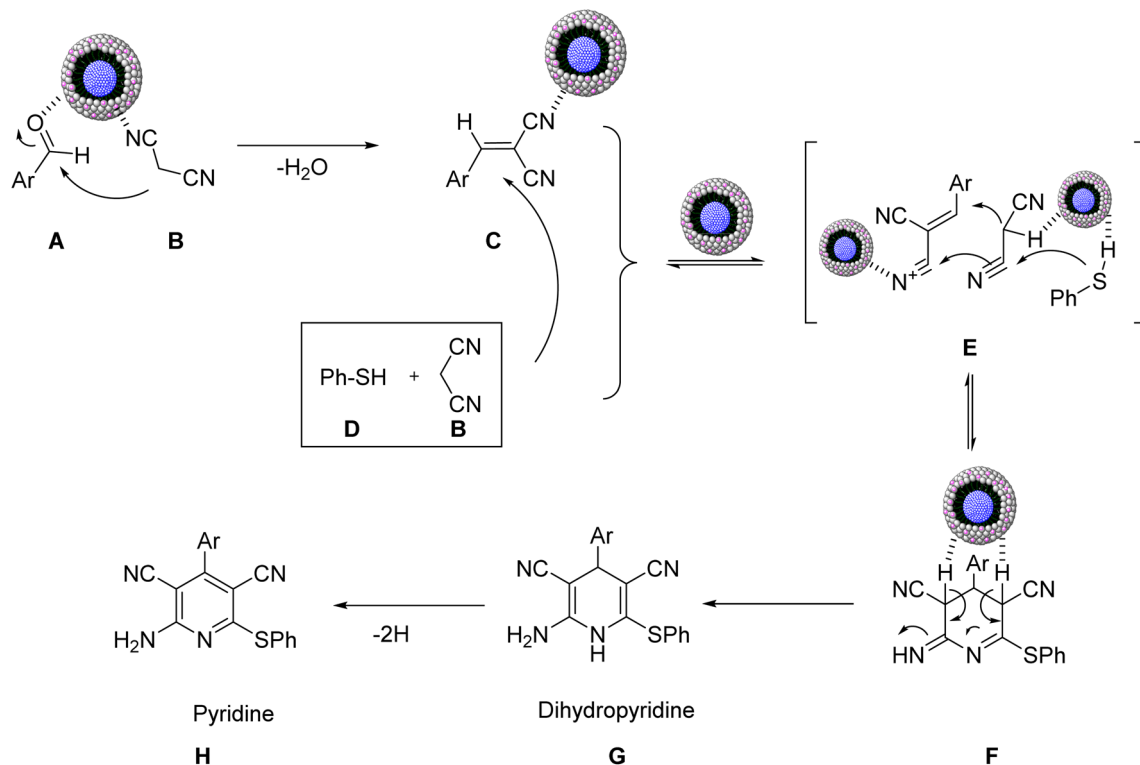


Fig. 10 (a) Reusability results of Ni^{II} -picolylamine/TCT/APTES@ SiO_2 @ Fe_3O_4 , (b) TEM image, and (c) size distribution of the reused catalyst.



Scheme 5 Gram-scale synthesis for the desired product **4b**.



Scheme 6 Plausible mechanism for the construction of substituted pyridine derivatives catalyzed by Ni^{II}-picolylamine/TCT/APTES@SiO₂@Fe₃O₄.

Conclusion

The synthesis of Ni^{II}-picolylamine/TCT/APTES@SiO₂@Fe₃O₄ was reported according to a convenient and simple four-step operation process. The as-prepared nanocatalyst was characterized by FT-IR, XPS, TGA, VSM, TEM, XRD, BET, FE-SEM, ICP-AES, and EDX analyses. The activity of the as-prepared nanocatalyst was investigated in the one-pot pseudo-four component reaction of malononitrile, thiophenol, and a variety of aldehyde derivatives under solvent-free conditions or EG at 80 °C, and the corresponding products were obtained in excellent yields. This method is safe and environmentally benign and offers various advantages, such as no use of column chromatography, easy workup procedure, multiple carbon–heteroatom and carbon–carbon bond formation, usage of green solvent, environmental friendliness, economical processing, high product yield, and easy separation of the catalyst from the reaction environment. The as-synthesized nanocatalyst indicated good reusability by employing a magnetic bar, with only small decreases in the yields of the reaction from 97% to 87%. Likewise, a negligible loss of Ni (1% leaching) was observed on the basis of ICP analysis after eight runs.

Author contributions

S. Rezayati and A. Ramazani conceived the idea and designed the research. S. Rezayati and F. Kalantari carried out the research. S. Rezayati analyzed the data. S. Rezayati wrote the

original draft. A. Ramazani reviewed the manuscript and editing. A. Ramazani was responsible for the funding acquisition.

Conflicts of interest

There are no conflicts to declare.

Acknowledgements

The present study, derived from PhD thesis by Sobhan Rezayati, was supported by Iran National Science Foundation INSF and the University of Zanjan.

References

- 1 R. S. Varma, *ACS Sustainable Chem. Eng.*, 2019, **7**, 6458–6470.
- 2 S. A. Nafiu, S. Shaheen Shah, A. Aziz and M. Nasiruzzaman Shaikh, *Chem.-Asian J.*, 2021, **16**, 1956–1966.
- 3 W. Wang, M. Luo, W. Yao, M. Ma, S. A. Pullarkat, L. Xu and P. H. Leung, *New J. Chem.*, 2019, **43**, 10744–10749.
- 4 B. Baruah and M. L. Deb, *Org. Biomol. Chem.*, 2021, **19**, 1191–1229.
- 5 Z. Ma, B. Zhao, Y. Gong, J. Deng and Z. Tan, *J. Mater. Chem. A*, 2019, **7**, 22826–22847.
- 6 H. Tian, S. Liu, Z. Zhang, T. Dang, Y. Lu and S. Liu, *ACS Sustainable Chem. Eng.*, 2021, **9**, 4660–4667.
- 7 Q. Yang, G. Pan, J. Wei, W. Wang, Y. Tang and Y. Cai, *ACS Sustainable Chem. Eng.*, 2021, **9**, 2367–2377.



- 8 M. Nasiruzzaman Shaikh, A. N. Kalanthoden, M. Ali, Md. A. Haque, Md. Abdul Aziz, M. M. Abdelnaby, S. K. Rani and A. Idris Bakare, *ChemistrySelect*, 2020, **5**, 14827–14838.
- 9 M. Nasiruzzaman Shaikh, Md. Abdul Aziz and Z. H. Yamani, *Catal. Sci. Technol.*, 2020, **10**, 6544–6551.
- 10 M. Nasiruzzaman Shaikh, A. Helal, A. N. Kalanthoden, B. Najjar, Md. Abdul Aziz and H. D. Mohamed, *Catal. Commun.*, 2019, **119**, 134–138.
- 11 M. Nasiruzzaman Shaikh, Md. Abdul Aziz, A. N. Kalanthoden, A. Helal, A. S. Hakeema and M. Bououdina, *Catal. Sci. Technol.*, 2018, **8**, 4709–4717.
- 12 J. P. K. Reynhardt, Y. Yang, A. Sayari and H. Alper, *Adv. Synth. Catal.*, 2005, **347**, 1379–1388.
- 13 A. N. Kalanthoden, Md. H. Zahir, Md. Abdul Aziz, B. Al-Najar, S. K. Rani and M. Nasiruzzaman Shaikh, *Chem.-Asian J.*, 2022, **17**, e202101195.
- 14 V. Polshettiwar, R. Luque, A. Fihri, H. Zhu, M. Bouhrara and J. M. Basset, *Chem. Rev.*, 2011, **111**, 3036–3075.
- 15 M. Gawande, A. Rathi, P. Branco and R. Varma, *Appl. Sci.*, 2013, **3**, 656–674.
- 16 M. Esmailpour, J. Javidi, F. N. Dodeji and M. M. M. Abarghoui, *Transition Met. Chem.*, 2014, **39**, 797–809.
- 17 S. Rezayati, Y. Ahmadi and A. Ramazani, *Inorg. Chim. Acta*, 2023, **544**, 121203.
- 18 R. Abu-Reziq, H. Alper, D. Wang and M. L. Post, *J. Am. Chem. Soc.*, 2006, **128**, 5279–5282.
- 19 M. Nasiruzzaman Shaikh, M. Bououdina, A. Azeez Jimoh, Md. Abdul Aziz, A. Helal, A. S. Hakeem, Z. H. Yamania and T. J. Kim, *New J. Chem.*, 2015, **39**, 7293–7299.
- 20 M. Nasiruzzaman Shaikh, Md. Abdul Aziz, A. Helal, M. Bououdina, Z. H. Yamani and T. J. Kim, *RSC Adv.*, 2016, **6**, 41687–41695.
- 21 A. Nasar Kalanthoden, Md. Hasan Zahir, Md. Abdul Aziz, B. Al-Najar, S. K. Rani and M. Nasiruzzaman Shaikh, *Chem.-Asian J.*, 2022, **17**, e202101195.
- 22 N. Griffete, F. Herbst, J. Pinson, S. Ammar and C. Mangeney, *J. Am. Chem. Soc.*, 2011, **133**, 1646–1649.
- 23 B. B. Toure and D. G. Hall, *Chem. Rev.*, 2009, **109**, 4439–4486.
- 24 E. Ruijter, R. Scheffelaar and R. V. Orru, *Angew. Chem., Int. Ed.*, 2011, **50**, 6234–6246.
- 25 A. Maleki, Z. Hajizadeh and R. Firouzi-Haji, *Microporous Mesoporous Mater.*, 2018, **259**, 46–53.
- 26 A. Maleki, M. Niksefat, J. Rahimi and R. Taheri-Ledari, *Mater. Today Chem.*, 2019, **13**, 110–120.
- 27 A. Maleki, R. Firouzi-Haji and Z. Hajizadeh, *Int. J. Biol. Macromol.*, 2018, **116**, 320–326.
- 28 S. B. Levy, M. N. Alekshun, B. L. Podlogar, K. Ohemeng, A. K. Verma, T. Warchol, B. Bhatia, T. Bowser and M. U. S. Grier, Patent Appl., 2005124678 A1 20050609, 2005.
- 29 T. R. K. Reddy, R. Mutter, W. Heal, K. Guo, V. J. Gillet, S. Pratt and B. Chen, *J. Med. Chem.*, 2006, **46**, 607–615.
- 30 M. T. Cocco, C. Congiu, V. Lilliu and V. Onnis, *Eur. J. Med. Chem.*, 2005, **40**, 1365–1372.
- 31 H. Chen, W. Zhang, R. Tam and A. K. Raney, PCT Int. Appl., WO 2005058315 A1, 20050630, 2005.
- 32 B. B. Fredholm, A. P. Ijzerman, K. A. Jacobson and K. N. Klotz, *J. Pharmacol. Rev.*, 2001, **53**, 527–552.
- 33 A. J. Herlt, R. W. Rickards and J. P. J. Wu, *Antibiot*, 1985, **38**, 516–518.
- 34 H. Wang, S. L. Yeo, J. Xu, X. Xu, H. He, F. Ronca, A. E. Ting, Y. Wang, V. C. Yu and M. M. Sim, *J. Nat. Prod.*, 2002, **65**, 721–724.
- 35 D. L. Boger, S. D. Burke, T. A. Engler, B. Fraser-Reid, M. N. Greco, P. Helquist, P. A. Jacobi, M. E. Jung, A. P. Kozikowski, S. E. Martin, W. R. Roush, A. B. Smith III, R. Tsang, D. R. Williams and T. Lindberg, ed. Academic Press, San Diego, 1988, **2**, 1.
- 36 E. S. Kim, *Drugs*, 2017, **77**, 2063–2070.
- 37 M. W. Beukers, L. C. W. Chang, J. K. von Frijtag Drabbe Künzel, T. Mulder-Krieger, R. F. Spanjersberg, J. Brussee and A. P. Ijzerman, *J. Med. Chem.*, 2004, **47**, 3707–3709.
- 38 L. C. W. Chang, J. K. von Frijtag Drabbe Künzel, T. Mulder-Krieger, R. F. Spanjersberg, S. F. Roerink, G. van den Hout, M. W. Beukers, J. Brussee and A. P. Ijzerman, *J. Med. Chem.*, 2005, **48**, 2045–2053.
- 39 S. Tu, B. Jiang, H. Jiang, Y. Zhang, R. Jia, J. Zhang, Q. Shao, C. Li, D. Zhou and L. Cao, *Tetrahedron*, 2007, **63**, 5406–5414.
- 40 M. Sridhar, B. C. Ramanaiah, C. Narsaiah, B. Mahesh, M. Kumaraswamy, K. R. R. Mallu, V. M. Ankathi and P. S. Rao, *Tetrahedron Lett.*, 2009, **50**, 3897.
- 41 M. L. Kantam, K. Mahendar and S. Bhargava, *J. Chem. Sci.*, 2010, **122**, 63–69.
- 42 S. Takale, J. Patil, V. Padalkar, R. Pisal and A. Chaskar, *J. Braz. Chem. Soc.*, 2012, **23**, 966–969.
- 43 R. Mamgain, R. Singh and D. S. Rawat, *J. Heterocycl. Chem.*, 2009, **46**, 69–73.
- 44 K. N. Singh and S. K. Singh, *ARKIVOC*, 2009, **xiii**, 153–160.
- 45 S. Shrinivas Kottawar, A. Shapi Siddiqui and R. Sudhakar Bhusare, *Heterocycl. Commun.*, 2012, **18**, 249–252.
- 46 B. C. Ranu, R. Jana and S. Sowmiah, *J. Org. Chem.*, 2007, **72**, 3152–3154.
- 47 N. M. Evdokimov, I. V. Magedov, A. S. Kireev and A. Konienko, *Org. Lett.*, 2006, **8**, 899–902.
- 48 A. Allahi and B. Akhlaghinia, *Phosphorus, Sulfur, and Silicon and the Related Elements*, 2021, **196**, 328–336.
- 49 B. Maleki, H. Natheghi, R. Tayebbe, H. Alinezhad, A. Amiri, S. A. Hossieni and S. M. Mahdi Nouri, *Polycyclic Aromat. Compd.*, 2020, **40**, 633–643.
- 50 M. R. Poor Heravi and F. Fakhr, *Tetrahedron Lett.*, 2011, **52**, 6779–6782.
- 51 J. Safaei-Ghomi and M. A. Ghasemzadeh, *J. Sulfur Chem.*, 2013, **34**, 233–241.
- 52 P. V. Shinde, S. S. Sonar, B. B. Shingate and M. S. Shingare, *Tetrahedron Lett.*, 2012, **53**, 4870–4872.
- 53 P. V. Shinde, V. B. Labade, B. B. Shingate and M. S. Shingare, *J. Mol. Catal. A: Chem.*, 2011, **336**, 100–105.
- 54 M. S. Su, X. J. Ji, B. B. Zhao, M. Tian and J. J. Ma, *J. Chem. Soc. Pak.*, 2015, **37**, 1130–1134.
- 55 F. Kalantari, S. Rezayati, A. Ramazani, H. Aghahosseini, K. Ślepokura and T. Lis, *ACS Appl. Nano Mater.*, 2022, **5**, 1783–1797.



- 56 F. Kalantari, A. Ramazani, M. R. Poor Heravi, H. Aghahosseini and K. Šlepokura, *Inorg. Chem.*, 2021, **60**, 15010–15023.
- 57 S. Rezayati, A. Ramazani, S. Sajjadifar, H. Aghahosseini and A. Rezaei, *ACS Omega*, 2021, **6**, 25608–25622.
- 58 S. Rezayati, F. Kalantari, A. Ramazani, S. Sajjadifar, H. Aghahosseini and A. Rezaei, *Inorg. Chem.*, 2022, **61**, 992–1010.
- 59 Y. Zhang, D. Li, M. Yu, W. Ma, J. Guo and C. Wang, *ACS Appl. Mater. Interfaces*, 2014, **6**, 8836–8844.
- 60 F. Wu, J. Tian, Y. Su, J. Wang, C. Zhang, L. Bao, T. He, J. Li and S. Chen, *ACS Appl. Mater. Interfaces*, 2015, **7**, 7702–7708.

